A case study on monitoring Potential Induced Degradation (PID) recovery in multi-crystalline modules

I M Kwembur[1], J L Crozier McCleland[1], F J Vorster[1] and E E van Dyk[1]

[1] Nelson Mandela University, Port Elizabeth, South Africa

E-mail: s21379446@mandela.ac.za

Abstract

Potential Induced Degradation (PID) causes significant module degradation leading to decreased power output in photovoltaic (PV) power plants. Many PV power plants are constructed using transformerless inverters and may be susceptible to issues associated with the galvanic connection between the PV configuration and the power grid. This increases the likelihood of a leakage current between the PV system`s active circuit and the ground. The resulting electric field causes sodium (Na^+) ions to drift to the cell and some at a certain concentration may diffuse into the PN junction creating shunting paths. The PID detection tools employed in this work are maximum power measurements, comparison of open circuit voltage (V_{oc}) at low irradiance (200 $W.m^{-2}$) and high irradiance (1000 $W.m^{-2}$) and Electroluminescence (EL) imaging at 10% of Short-circuit current (I_{sc}). These techniques are used to assess the degree of PID and to monitor the module recovery. This work explores two recovery methods for PID affected modules, forced recovery and natural recovery. Forced recovery involves reverse biasing the module terminals for a few hours while natural recovery, modules are left unbiased for several months. This yields a maximum power recovery of approximately 95% and 94% for forced and natural recovery respectively. These techniques are used to assess the degree of PID and to monitor recovery. This paper demonstrates that PID recovery on modules depends on two mechanisms, viz. drift or diffusion, or combined.

1. Background

Photovoltaic (PV) solar power is a promising renewable source due to the abundance and inexhaustible nature of solar energy. Most of the first solar power plants to be constructed were fitted with high frequency transformers between the grid and PV system resulting in galvanic isolation [1]. This came at a cost since transformers are expensive, large and results in power conversion losses due to the several levels of conversion [2]. To solve these issues transformerless inverters were deployed with topologies that attempt to maintain the required galvanic isolation between the PV system and the power grid [1]. Inadequate galvanic isolation, however, made the PV power plants vulnerable to leakage current flowing between the PV active circuit and the ground resulting in potential induced degradation (PID) [1]. The electric field that developed between the module active circuit and the frame causes Na^+ ions (present in soda lime glass) [3] to migrate through the encapsulation to the surface of the cell and in some cases, when a sufficient concentration is attained, Na^+ ions are caused to diffuse into the PN junction [4]. The

accumulation of Na^+ ions in the PN junction results in a significant shunting leading to a decrease in shunt resistance (R_{sh}) and an increase in series resistance (R_s) which in turn, results in a decreased module power output [5]. The module closer to the negative side of the string (-V) are often more affected in comparison to modules on the positive side of the string (+V) because they are at the higher negative potential in relation to the ground [6]. The extent of PID damage depends on, the system voltage (potential between the active circuit and the earthed frame), humidity levels [7], ambient temperature [3], type of the glass used in module fabrication [8] and resistivity of the solar cell encapsulation [6].

Detection of PID shunted cells on a module is made possible by way of Electroluminescence (EL) imaging [9]. The EL imaging set up comprises of EL camera, programmable power supply and computer controls. EL imaging involves forward biasing the module, while the EL camera is placed at some optimised distance from the front surface of the module in a dark environment to eliminate interference from stray light. Under normal conditions, cells are detected with uniform brightness except inter-cell spaces, busbars and dark sports within the cells which appear darker [10]. For a module that has PID, the EL brightness varies depending on the degree of shunting, such cells or regions appear dark. The variation in brightness of the cell is commensurate to the number of minority charge carriers flowing into individual cells in a module. For PID affected cells the number of minority charge carriers are reduced due to increased R_s resulting in the dark appearance of PID affected cells [11].The main objective of this work is to induce PID in modules and compare two PID recovery procedures, (i) natural recovery and ii) reverse polarization on several module samples.

2. Modelling module current leakage pathways

In a typical PV system, a high electric potential difference between an active circuit and the aluminium frame induces a leakage current to flow through sections of the PV module. In a standard p-type crystalline silicon module seven current leakage pathways can be described and are depicted in figure 1. The pathways are; 1) along the glass surface, 2) through the glass substrate, 3) through the interface between the glass and the encapsulant, 4) through the encapsulation, 5) through the interface between the encapsulation and the back sheet, 6) through the back sheet substrate and 7) along the surface of the back sheet [3, 4]. For n-type modules, the PID stress set up is reversed biased in relation to that of figure 1.

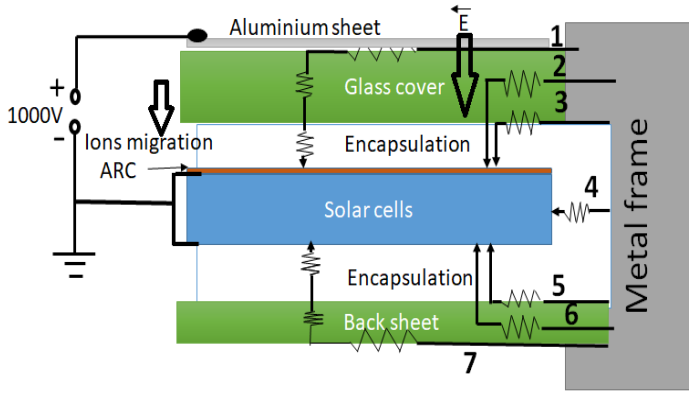

Figure 1. A cross section of mc-Si PV module constructed to indicate current modelled current leakage: 1) along the glass surface, 2) through the glass substrate, 3) through the interface between glass and the encapsulation, 4) through the encapsulation substrate, 5) through the interface between the back encapsulation and the back sheet, 6) through the back sheet and 7) along the back sheet surface [3].

The magnitude of the leakage current increases with an increase in humidity [7], as such the leakage current is high in the morning owing to dew condensation on the glass surface in the morning hours. On days with low humidity, the conductivity is limited to the edges of the modules and not the surface as it would be the case for high humidity. This explains why cells along the frame are highly susceptible to PID. Over a long period of time, moisture may ingress into the module resulting in reduced encapsulant bulk resistivity which may enhance PID progression. In extreme humidity conditions in case of modules fabricated with EVA encapsulation, acetic acid may develop resulting corrosive irreversible PID [7].

3. Experimental set and procedure

3.1 PID induction in multi-crystalline modules

In this study five PV modules were used, four 60-cell multi-crystalline modules (X, A, B, C) and a 72-cell multi-crystalline module (D). The five modules from different manufacturers were subjected to PID stressing by applying a bias voltage of 1000V for 24 hours while placed in an environmental chamber that was kept at 35 ± 1 ºC, with relative humidity < 40% RH throughout the induction period. Biasing was achieved by applying a positive voltage to either a 3 mm thick aluminium plate resting on the entire surface of the module's cover glass without touching the frame as illustrated in figure 1, or to the frame itself. The negative voltage was connected to the shorted module connector terminals.

3.2 PID detection light IV measurements and EL imaging

PID is confirmed by a drop in power measured by an indoor solar simulator. The measurements are taken when the simulator is set at STC (standard test condition of 25ºC temperature, Irradiance of 1000 $W.m^{-2}$). For purposes of PID detection the second power measurement was taken when irradiance is set at 200 $W.m^{-2}$ and temperature of 25ºC. This is because at low irradiance, PID affected module experience greater carrier losses to the shunted paths with reduction in photocurrent as compared to 1000 $W.m^{-2}$ where the carrier losses go undetected because of abundance of photocurrents [3].

In addition to power loss, PID in a module can be detected from power measurements by comparing the open circuit voltage (V_{oc}) obtained at solar irradiance of 1000 $W.m^{-2}$ and 200 $W.m^{-2}$. If the V_{oc} drops by more than 10% between 200 $W.m^{-2}$ and 1000 $W.m^{-2}$, the module may have PID and may experience PID shunting [6]. For module X used in this section, the V_{oc} drop is 7.9% before PID and 36.2% after PD stress (see table 1). The increase in the low-high irradiance V_{oc} difference may be indicative of the presence of PID shunting otherwise, for any other PV performance limiting defect the V_{oc} ratio may be within a small increase. PID affected cells on a module in an EL image appear darker/less bright as compared to the rest as observed in figure 3 and figure 5. EL images in this work were recorded at 10% of I_{sc} because PID shunted cells appear distinctively less bright as compared to those taken at I_{sc}[10].

Table 1: Table of V_{oc} and P_{mpp} taken at 1000 $W.m^{-2}$ and 200 $W.m^{-2}$ irradiance for module X.

	Before PID		After PID	
Irradiance	1000 $W.m^{-2}$	200 $W.m^{-2}$	1000 $W.m^{-2}$	200 $W.m^{-2}$
V_{oc} (V)	37.3	34.3	36.0	22.9
P_{mpp} (W)	230.0	40.5	149.6	12.4

3.3 Module recovery Procedure

It is possible that modules can recover from induced PID by reversing the degradation caused by PID shunting [3]. This was done in two ways; 1) forced reverse polarity of a module for 120 minutes or 2) by way of unbiased natural recovery in the dark at the open circuit over a period up to 12 months at room temperature. The recovery percentage is calculated based on the initial power measurements of the module. The recovery procedure was monitored by periodically measuring maximum power output using a class AAA of a solar simulator, (spectral mismatch of 0.75-1.25 times the ideal spectral range, spatial uniformity ≤ 2% and temporal instability on measurements of 0.5% on short term and < 2% on the long term) [12]. EL images are recorded at a current corresponding to 10% of I_{sc}.

4. Results and Discussion

4.1 Module recovery

The modules were subjected to PID stress and evaluated using the techniques discussed in section 3.2. The modules showed varying degrees of PID and the characteristics are summarized in table 2. In the table, the initial and degraded power of the modules is listed together with the associated % drop in power (the ratio of the difference between initial and final power and initial power), post recovery power and % recovery (ratio of power recovered to power lost). The rate of the recovery is determined based on recovery period which was quoted either as per minute or per day, depending on the duration of recovery time. Module A underwent forced reversed biased recovery and after 120 minutes the module power recovered up to 94.8% of the degraded power. Module B was subjected to natural recovery at room temperature in the dark at open circuit voltage and after 8 months the power recovery level was 94.0% of the degraded power. Module C which belongs to the same class as module A underwent extreme PID, with a power loss of 88.5%. After 7 months of natural recovery, the module has recovered 45.1% of the lost power. Module D degraded by 18.3% and underwent natural recovery for a period of 12 months with 74.6% recovery, making its recovery relatively slow compared to the other modules.

Table 2: Module characteristics of modules subjected to PID stress.

Module	Initial P_{mpp} (W)	Post PID stress P_{mpp} (W)	P_{mpp} drop (%)	Duration	Post recovery P_{mpp} (W)	P_{mpp} recovery (%)	Rate of recovery	Type of Recovery
A	233.9	148.7	36.4	120 minutes	229.5	94.8	0.67 $W.min^{-1}$	Reverse Polarization
B	265.9	187.1	29.6	8 months	261.2	94.0	0.31 $W.day^{-1}$	Natural
C	229.5	26.1	88.5	7 months	116.2	45.1	0.44 $W.day^{-1}$	Natural
D	294.4	240.5	18.3	12 months	280.9	74.6	0.11 $W.day^{-1}$	Natural

In addition to assessing PID recovery based on power measurement, EL images are a good indicator of recovery. The PID and subsequent recovery of modules A and B serve to illustrate this for excessive degradation and recovery via two different methods. Figures 2 and 4 show the respective I-V curve measurements for Modules A and B, taken before PID, after PID and after PID recovery. Figures 3 and 5, show the EL images for modules A and B, taken before PID, after PID and after PID recovery. From figures 2 and 4, the I-V curves show that modules have recovered substantially, but not to initial power level, although the curves appear to overlap. The EL images shown in figures 3 and 5, exhibits the expected checkerboard pattern of varying luminescence with the cells affected by PID appearing dark, and the subsequent absence of this pattern in the images after recovery.

The module recovery may not be 100% because Na^+ ions may not have been completely migrated from defect sites within the PN junction. In the case of natural recovery procedure, the procedure is slow since it only depended on diffusion as the mechanism to cause migration of Na^+ ions from the defect sites within the PN junction and cell surface. Forced recovery is quick since it combines both drift and diffusion of sodium ion Na^+ ions hence it is quick taking approximately 120 minutes (module A) as compared to 8 months in the case of natural recovery (module B). Different PV manufacturers use different types of encapsulation with varied resistivity properties the same applies to the glass cover [13]. In addition, different mechanisms have been used in module fabrication to limit PID progression in modules, as such modules will exhibit a varied response to PID progression effect and power recovery [14]. PID shunting can easily be detected at infancy using EL imaging taken at low current and power measurements at low irradiance.

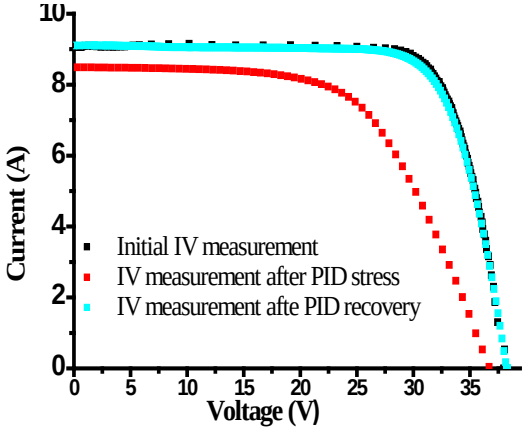

Figure 2. Light I-V measurements for Module A.

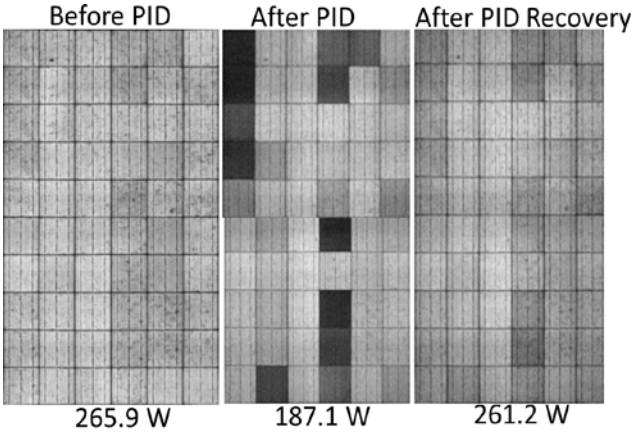

Figure 3. EL-images of module A recorded 10% I_{sc} with the measured P_{mpp} listed.

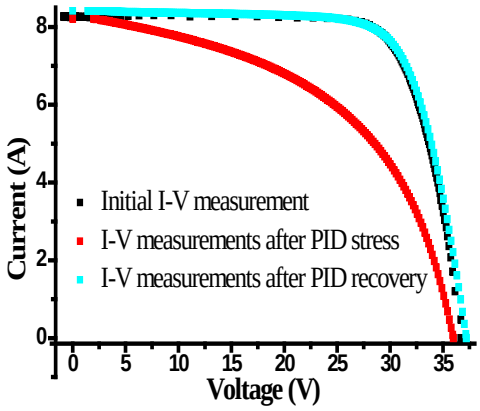

Figure 4. Light I-V measurements for Module B.

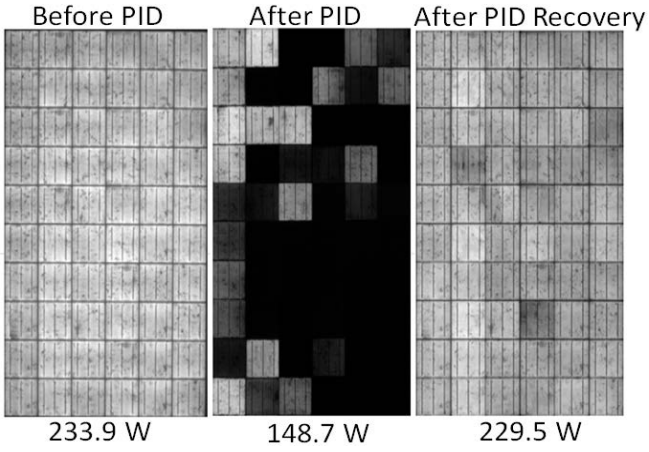

Figure 5. EL-images of module B recorded at 10% of I_{sc} with the measured P_{mpp} listed.

5. Conclusion

PID if left undetected can greatly affect the performance of modules in a string, hence need to detect and undertake module recovery procedures. PID in modules is caused when an electric field between the frame and active circuit of the PV modules causes a leakage current to flow. In the process, Na^+ ions are forced to drift from the glass to the cells and at the right concentration, the Na^+ ions are forced to diffuse into PN junction resulting in increased $R_{s.}$. Under low irradiance PID affected cells generate less charge carriers because of increased recombination resulting in less power output as compared to the PID free cells. The PID affected cells also appear less bright in comparison to the rest of the cells in an EL image. EL imaging and power measurement at low irradiance are two complementary methods used to successfully detected presence of PID in a PV module. Module power recovery procedures by way of forced recovery over a short period of time or unbiased natural conditions in the dark over a long period of time were deployed. The PID recovery occurred because Na^+ ions were forced to migrate from the cells back to the glass by a strong electric field in reverse to the PID inducing electric field and diffusion over a long period of time for the unbiased method. In both the procedures more than 94% of power lost was recovered in modules A and B. However, incomplete Na^+ ions removal from the PN

junction may be responsible for not attaining 100% P_{mpp} recovery. Solar PV power plant operators can employ a simple procedure to partly recover modules affected by PID by disconnecting the modules in situ, effectively keeping them under open circuit condition for an extended period of time that can be optimally determined by the solar plant operator.

Acknowledgements
The authors gratefully acknowledge the South African National Research Foundation (NRF), PVinsight (Pty) Ltd, National Laser Centre (NLC), African Laser Centre (ALC), the South African Department of Science and Technology (DST), ESKOM and Nelson Mandela University (NMU) for the financial support and providing necessary facilities for research.

References

[1] Shayestegan M. Overview of grid-connected two-stage transformer-less inverter design. *J Mod Power Syst Clean Energy* 2018; **6**: 642–655.
[2] Kumar LA, Kumar S. Design and Analysis of Highly Efficient and Reliable Single-Phase Transformerless Inverter for PV Systems. *Int J Energy Power Eng* 2014; **8**: 1405–1410.
[3] Luo W, Khoo YS, Hacke P, Naumann V, Lausch D, Harvey SP, Singh JP, et al. Potential-induced degradation in photovoltaic modules: a critical review. *Energy Environ Sci* 2017; **10**: 43–68.
[4] Luo W, Hacke P, Singh JP, Chai J, Wang Y, Ramakrishna S, Aberle AG, et al. In-Situ Characterization of Potential-Induced Degradation in Crystalline Silicon Photovoltaic Modules Through Dark I-V Measurements. *IEEE J Photovoltaics* 2017; **7**: 104–109.
[5] Pingel S, Frank O, Winkler M, Oaryan S, Geipel T, Hoehne H, Berghold J. Potential Induced Degradation of Solar Cells and Panels. In: *35th IEEE PVSC.*, pp. 2817–2822.
[6] Schwark M, Berger K, Ebner R, Ujvari G, Hirschl C, Neumaier L, Muhleisen W. Investigation of potential induced degradation (PID) of solar modules from different manufacturers. *IECON Proc (Industrial Electron Conf* 2013; **8**: 8090–8097.
[7] Hoffmann S, Michael K. Effect of humidity and temperature on the potential-induced degradation. *Prog Photovolt Res Appl* 2014; **22**: 173–179.
[8] Burrows K, Fthenakis V. Glass needs for a growing photovoltaics industry. *Sol Energy Mater Sol Cells* 2015; **132**: 455–459.
[9] Fuyuki T, Kitiyanan A. Electroluminescence Characterization of Crystalline Silicon Solar Cells. *Appl Phys A Mater Sci Process* 2009; **96**: 189–196.
[10] Kwembur IM, Crozier McCleland JL, van Dyk EE, Vorster FJ. Detection of Potential Induced Degradation in mono and multi-crystalline silicon photovoltaic modules. *Phys B Condens Matter* 2020; **581**: 1–6.
[11] International Electrotechnical Commission. *Electroluminescence of photovoltaic modules*. IEC TS 60904-13, Geneva, www.iec.ch (2019).
[12] Droz C, Fakhfouri V, Pelet Y, Roux J, Peguiron N, Beljean P-R. Evaluation of Commercial Large Area Solar Simulator: Features Exceeding the IEC Standard Class AAA. In: *25th European Photovoltaic Solar Energy Conference and Exhibition / 5th World Conference on Photovoltaic Energy Conversion, 6-10 September 2010, Valencia, Spain*, pp. 3884–3888.
[13] Koch S, Berghold J, Okoroafor O, Krauter S, Grunow P. Encapsulation Influence on the Potential Induced Degradation of Crystalline Silicon Cells with Selective Emitter Structures. In: *27th European Photovoltaic Solar Energy Conference and Exhibition*. Frankfurt, Germany, pp. 1991–1995.
[14] S. Pingel, Janke S, O. Frank. Recovery Methods for Modules Affected by Potential Induced Degradation (PID). In: *27th European Photovoltaic Solar Energy Conference and Exhibition*, pp. 3379–3383.